Journal of Clinical and Translational Hepatology **2023** vol. 11(1) | 97–109
DOI: 10.14218/JCTH.2021.00391

Original Article

MALAT1-mediated EZH2 Recruitment to the GFER Promoter Region Curbs Normal Hepatocyte Proliferation in Acute Liver Injury

Li Chen[1#*], Xintong Kang[2#], Xiujuan Meng[3], Liang Huang[2], Yiting Du[4], Yilan Zeng[2] and Chunfeng Liao[5]

[1]Department of Infectious Diseases, The Third Xiangya Hospital of Central South University, Changsha, Hunan, China; [2]Department of Hepatology, Public Health Clinical Center of Chengdu, Chengdu, Sichuan, China; [3]Hospital-Acquired Infection Control Center, Xiangya Hospital Central South University, Changsha, Hunan, China; [4]Department of Emergency, Chengdu Women's and Children's Central Hospital, Chengdu, Sichuan, China; [5]Department of Cardiovascular Medicine, The First Hospital of Changsha, Changsha, Hunan, China

Received: 6 September 2021 | **Revised:** 12 November 2021 | **Accepted:** 4 March 2022 | **Published:** 15 April 2022

Abstract

Background and Aims: The goal of this study was to investigate the mechanism by which the long noncoding RNA MALAT1 inhibited hepatocyte proliferation in acute liver injury (ALI). ***Methods:*** Lipopolysaccharide (LPS) was used to induce an ALI cellular model in HL7702 cells, in which lentivirus vectors containing MALAT1/EZH2/GFER overexpression or knockdown were introduced. A series of experiments were performed to determine their roles in liver injury, oxidative stress injury, and cell biological processes. The interaction of MALAT1 with EZH2 and enrichment of EZH2 and H3K27me3 in the GFER promoter region were identified. Rats were treated with MALAT1 knockdown or GFER overexpression before LPS induction to verify the results derived from the *in vitro* assay. ***Results:*** MALAT1 levels were elevated and GFER levels were reduced in ALI patients and the LPS-induced cell model. MALAT1 knockdown or GFER overexpression suppressed cell apoptosis and oxidative stress injury induced cell proliferation, and reduced ALI. Functionally, MALAT1 interacted directly with EZH2 and increased the enrichment of EZH2 and H3K27me3 in the GFER promoter region to reduce GFER expression. Moreover, MALAT1/EZH2/GFER was activated the AMPK/mTOR signaling pathway. ***Conclusion:*** Our study highlighted the inhibitory role of reduced MALAT1 in ALI through the modulation of EZH2-mediated GFER.

Citation of this article: Chen L, Kang X, Meng X, Huang L, Du Y, Zeng Y, *et al*. MALAT1-mediated EZH2 Recruitment to the GFER Promoter Region Curbs Normal Hepatocyte Proliferation in Acute Liver Injury. J Clin Transl Hepatol 2023;11(1):97–109. doi: 10.14218/JCTH.2021.00391.

Keywords: MALAT1; EZH2; GFER; H3K27me3; Methylation; Acute liver injury.

Abbreviations: ADILI, acute drug-induced liver injury; ALI, acute liver injury; ALP, alkaline phosphatase; ALT, alanine aminotransferase; AMPK, adenosine monophosphate-activated protein kinase; AST, aspartate aminotransferase; LDH, lactic dehydrogenase; LncRNA, long noncoding RNA; LPS, lipopolysaccharide; NC, negative control.

[#]Contributed equally to this research.

[*]**Correspondence to:** Li Chen, Department of Infectious Diseases, The Third Xiangya Hospital of Central South University, No.138, Tongzipo Road, Yuelu District, Changsha, Hunan 410013, China. ORCID: https://orcid.org/0000-0003-2385-2858. Tel: +86-13755192409, E-mail: chenli198007@163.com

Introduction

Acute liver injury (ALI) is a pernicious clinical condition marked by rapid hepatocyte dysfunction and defects in patients with or without a history of liver disease.[1] Hepatitis viruses, drugs, immunologic injury and other hepatotoxic factors cause significant hepatocyte death, ultimately inducing ALI or even acute liver failure (ALF).[2] Increases in aspartate aminotransferase (AST) and alanine aminotransferase (ALT) are used to identify the likelihood of ALI.[3,4] Currently, immunosuppressors, antiviral agents, bioartificial livers, and liver transplantation are available treatment options for ALI.[5] For patients with ALF and acute-on-chronic liver failure, the only definitive option is liver transplantation when there is a poor prognosis.[6] Of note, the prognosis is often made worse by ineffective treatment, high cost, risk of organ rejection, limited liver donors, and severe treatment-related adverse effects.[5,7] Under the circumstances, it is imperative to develop novel treatment strategies to prevent ALI.

Long noncoding (lnc)RNAs are transcripts >200 nucleotides that are dysregulated in liver disease and are considered biological markers for the diagnosis, prognosis, and treatment.[8,9] Abnormal expression of MALAT1 has been identified in rodent models and patients with acute kidney injury.[10] Interestingly, downregulation of MALAT1 blocks hypoxia/reoxygenation-induced hepatocyte apoptosis and limits the release of lactic dehydrogenase (LDH).[11] Knockdown of MALAT1 improves the outcome of lipopolysaccharide (LPS)-induced acute lung injury and suppresses apoptosis of human pulmonary microvascular endothelial cells.[12] Moreover, MALAT1 recruits the histone methyltransferase EZH2 to the microRNA (miR)-22 promoter region, thus inhibiting the expression of miR-22.[13] Furthermore, MALAT1 recruits EZH2 to the promoter region of ABI3BP to downregulate its expression and modulate H3K27 methylation in gallbladder cancer cells.[14] Notably, regulation of methylation plays an essential role in the deterioration and management of ALI.[15,16] In addition, GFER encodes augmenter of liver regeneration (ALR) a protein that specifically supports liver regeneration.[17] Transient knockdown of GFER has been found to promote cell death and reduce cell proliferation in liver tissue.[18] We hypothesized that GFER is a downstream

Table 1. GAPDH, MALAT1, and GFER primers

Name of primer	Sequences
GAPDH-F	AATGGGCAGCCGTTAGGAAA
GAPDH-R	GCGCCCAATACGACCAAATC
MALAT1-F	GCTCTGTGGTGTGGGATTGA
MALAT1-R	GTGGCAAAATGGCGGACTTT
GFER-F	AAGCCTGACTTCGACTGCTC
GFER-R	CAAACCTAAGAGGGGCAGGG

F, forward; R, reverse.

gene regulated by MALAT1 in ALI. The study aim was to elucidate the role and potential mechanism of MALAT1 in LPS-induced ALI. To that end, animal and cellular models of ALI were established using LPS, and the severity of ALI, apoptosis and proliferation were assessed.

Methods

Clinical sample collection

This study included 26 patients with acute drug-induced liver injury (ADILI) who were hospitalized in the liver disease department of The Third Xiangya Hospital of Central South University and 19 healthy people from the physical examination clinic of The Third Xiangya Hospital of Central South University. The diagnostic criteria of ADILI were based on the guidelines for the diagnosis and treatment of drug-induced liver injury of the 17th National Conference on Viral Hepatitis and Hepatology of the Chinese Medical Association in 2015 and a Roussel Uclaf Causality Assessment Method (RUCAM) scale score of >8 points.[19] Patients were excluded if they had viral hepatitis B or C or other types of viral hepatitis, autoimmune liver disease, alcoholic liver disease, nonalcoholic fatty liver disease, cholestatic disease, or inherited metabolic liver disease. Peripheral blood was selected for clinical research in this study because liver biopsies were not performed. Approximately 4 mL of peripheral blood was collected in the morning after overnight fasting, placed in a serum tube, centrifuged at 4,000 rpm at 4°C for 10 m, and stored at −80°C until. use. This study complied with the Declaration of Helsinki and was approved by the ethics committee of The Third Xiangya Hospital of Central South University. All patients signed an informed consent form (No. 22014). Patient information is shown in Table 1.

Hepatocyte culture and treatment

HL7702 human hepatocyte cells were provided by Cell Bank of Chinese Academy of Science and maintained in Dulbecco's modified Eagle's medium (Gibco, Grand Island, NY, USA) containing 10% fetal bovine serum plus 1% streptomycin-penicillin and cultured in a 37°C incubator with 5% CO_2. Hepatocytes were induced by 1 μg/mL LPS (Sigma-Aldrich, St Louis, MO, USA) for 16 h in a 5% CO_2 atmosphere at 37°C to induce ALI. In some cases, hepatocytes were cultured with an adenosine monophosphate-activated protein kinase (AMPK) inhibitor (10 μM, Compound C; Sigma-Aldrich) for 1 h before LPS induction.

HL7702 cells were seeded in culture plates and transfected with MALAT1 overexpression vector (oe-MALAT1), MALAT1 knockdown vector (sh-MALAT1, 20 μL, viral titer 5×10^8 TU/mL), EZH2 overexpression vector (oe-EZH2, 20 μL, viral titer 5×10^8 TU/mL), EZH2 knockdown vector (sh-EZH2, 20 μL, viral titer of 5×10^8 TU/mL), GFER overexpression vector (oe-GFER, 20 μL, viral titer of 3×10^8 TU/mL), GFER knockdown short hairpin vector (sh-GFER, 20 μL, viral titer of 5×10^8 TU/mL) or the corresponding negative controls (oe-NC and sh-NC) (20 μL, 3×10^8 TU/mL). Lentivirus vectors used for gene overexpression (LV5-GFP) or knockdown (pSIH1-H1-copGFP) were provided by GenePharma (Shanghai, China). Each experiment was conducted in triplicate. LPS induction was performed in HL7702 cells 24 h after transfection.

Animals

The animal procedures in this study were approved by the Ethics Committee of The Third Xiangya Hospital of Central South University (No. 22014) and followed the guidelines of the National Institutes of Health. Forty-two Sprague-Dawley rats 7–8 weeks of age, and 200–250 g (Shanghai Laboratory, Animal Research Center, Chinese Academy of Science) were fed under pathogen-free conditions and kept in a 12 h light/dark cycle and 60–65% humidity. The rats were allowed free access to food and water.

The rat ALI model was induced by intraperitoneal injection of 10 mg/kg LPS (Sigma-Aldrich), with normal saline treatment as the control. The model was maintained for 6 h before sh-MALAT1 (5×10^8 TU/mL, 300 μL/rat) or oe-GFER (3×10^8 TU/mL, 300 μL/rat) was introduced into rats through intravenous injection in tails for MALAT1 knockdown or GFER overexpression, with sh-NC (3×10^8 TU/mL, 300 μL/rat) or oe-NC (3×10^8 TU/mL, 300 μL/rat) as the negative control. The 42 rats were randomly divided into seven groups of six rats each, including normal controls, and saline (administration of an equal volume of normal saline), LPS (intraperitoneal injection of 10 mg/kg LPS for 6 h modelling), LPS + sh-NC group (intravenous injection of sh-NC in the tail vein 42 h before LPS induction, followed by intraperitoneal injection of 10 mg/kg LPS for 6 h modelling), LPS + sh-MALAT1 (injection of sh-MALAT1 in the tail vein 42 h before LPS induction, followed by intraperitoneal injection of 10 mg/kg LPS for a 6-h modelling), LPS + oe-NC group (injection of oe-NC in the tail vein 42 h before LPS induction, followed by intraperitoneal injection of 10 mg/kg LPS for a 6-h modelling), and LPS + oe-GFER (injection of oe-GFER in the tail vein 42 h before LPS induction, followed by intraperitoneal injection of 10 mg/kg LPS for a 6-h modelling). All animals were sacrificed to collect serum and liver tissue 48 h after modelling for 6 h and injection of lentivirus vectors.

Quantitative real-time polymerase chain reaction (qRT-PCR)

RNA extraction of cells or tissues was carried out using TRIzol (Invitrogen, Carlsbad, CA, USA) followed by detection of RNA concentration and purity. Qualified RNA samples were adjusted to an appropriate concentration and then reverse-transcribed using random primers and a reverse transcription kit (TaKaRa, Tokyo, Japan) following the manufacturer's instructions. Gene expression was quantified by fluorescence qRT-PCR (LightCycler 480; Roche, Indianapolis, IN, USA), and was carried out following the manufacturer's instructions (SYBR Green Mix; Roche Diagnostics). In brief, cDNA templates were predenatured at 95°C for 5 m, denatured at 95°C for 10 s, annealed at 60°C for 10 s and finally extended at 72°C for 20 s, followed by 40 cycles of cycling. Each qPCR assay was performed with three replicates. The

Table 2. Patient characteristics

	Normal (*n*=19)	ADILI (*n*=26)
Age (years)	52.56±1.85	56.46±1.42
Sex (male/female)	11/15	8/11
ALT (U/L)	27.45±3.74	410.53±114.02***
AST (U/L)	27.12±3.51	316.74±84.85***
γ-GT (U/L)	24.22±4.56	285.84±76.43***
ALP (U/L)	85.16±12.35	153.21±21.85*
TBil (μmol/L)	13.51±2.13	35.51±2.13*
INR	0.95±0.11	1.15±0.23
RUCAM score	0.67±0.96	9.27±1.84*

*p<0.05, ***p<0.001 vs. the normal group. ADILI, acute drug-induced liver injury; ALT, alanine transaminase; AST, aspartate aminotransferase; γ-GT, gamma-glutamyl transpeptidase; ALP, alkaline phosphatase; TBil, total bilirubin; INR, international normalized ratio; RUCAM, Roussel Uclaf Causality Assessment Method.

relative expression of GFER and MALAT1 was determined by the $2^{-\Delta\Delta Ct}$ method with GAPDH as the reference gene. The primer sequences for GAPDH, MALAT1, and GFER are shown in Table 2.

Western blot assays

Cells or tissues were lysed in RIPA lysis buffer and centrifuged for protein extraction. Protein concentration was detected with a bicinchoninic acid assay kit (Beyotime Biotechnology, Shanghai, China) to ensure equal loading volume of protein. The corresponding volume of protein was homogenized with loading buffer (Beyotime) and then denatured for 3 m in a boiling water bath. Proteins were separated on 10% sodium dodecyl-sulfate polyacrylamide gel electrophoresis (SDS-PAGE) gels following the kit (Beyotime) manufacturer's instructions. Briefly, the protein was electrophoresed at 80 V, and then the voltage was switched to 120 V for 1–2 h. After protein separation, membrane transfer was performed in an ice bath at 300 mA for 60 m. Then, the membranes were rinsed in a washing solution for 1–2 m, followed by blocking at room temperature for 60 m or at 4°C overnight. Incubation with primary antibodies against rabbit anti-human GAPDH (1:1,000; Cell Signaling, Boston, MA, USA), GFER (1:500; Santa Cruz Biotechnology, Dallas, TX, USA), p-mTOR (Ser2448 1:1,000; Cell Signaling Technology), mTOR (1:1,000; Cell Signaling Technology), p-AMPK (Thr172 1:1,000; Cell Signaling Technology), AMPK (1:1,000; Cell Signaling Technology), H3K27me3 (1:1,000; Abcam, Cambridge, UK), or EZH2 (1:500; Abcam) performed at room temperature on a shaking table for 1 h. After incubation, the membranes were washed three times for 10 m each and then incubated with horseradish peroxidase-labeled goat anti-rabbit IgG (1:5,000; Beijing ComWin Biotech Co., Ltd., Beijing, China) for 1 h at room temperature. Before color development, the membranes were washed three times for 10 m each. A chemiluminescence imaging system (Bio-Rad, Hercules, CA, USA) was used to visualize the membranes.

Assay of AST, ALT and LDH

The culture supernatant of HL7702 cells or rat serum was collected for liver function testing. AST, ALT, and LDH were assayed with kits following the manufacturer's (Sigma-Aldrich, Merck KGaA, Darmstadt, Germany) instructions.

Cell counting kit (CCK)-8 assay

Twenty-four hours after transfection, 100 μL of the cell suspension was seeded into a 96-well plate, with three replicates for each sample. Cells were cultured in an incubator for 24, 48, or 72 h, 10 μL of CCK-8 reagent (Dojindo, Tokyo, Japan) for 3 h, and absorbance was determined at 450 nm.

Ethynyl-deoxyuridine (EdU) staining

Cells (1×10^5 cells/well) were transferred to 96-well plates and cultured for 2 h with 100 μL EdU stain (5 μM; Sigma-Aldrich, Merck KGaA). The cells were then immobilized in 50 μL fixation buffer for 30 m. After removing the buffer, the cells were incubated with 50 μL glycine (2 mg/mL) for 5 m and washed with 100 μL phosphate buffered saline (PBS). After culture with 100 μL of permeabilization buffer and washing in 100 μL PBS, the cells were incubated with 100 μL of 1× Apollo solution in the dark for 30 m. Finally, the cells were cultured with 100 μL diamidino-phenylindole at room temperature for 5 m away from light and washed in 100 μL PBS, followed by observation by fluorescence microscopy (Olympus, Tokyo, Japan).

Terminal deoxynucleotidyl transferase dUTP nick end labeling (TUNEL) assay

Collected cells were fixed in 4% paraformaldehyde for 30 m and then in 70% cold alcohol for 15 m. The cells were then incubated with PBS containing 0.3% Triton X-100 at room temperature for 5 m and incubated with TUNEL solution (Beyotime) for 60 m at 37°C. After washing in PBS three times, the cells were blocked with an antifade reagent and observed by fluorescence microscopy. The cell nuclei were stained with diamidino-phenylindole and apoptosis (%)=(TUNEL-positive cells/total cells)×100.

Rats were sacrificed to collect liver tissues, which were fixed in 10% neutral buffer formalin (Beijing Solarbio Science & Technology Co., Ltd., Beijing, China) for 24 h, dehydrated, and embedded in paraffin. After being sliced into 4 μm serial sections, the tissue was dewaxed with xylene and dehydrated in an alcohol gradient. A TUNEL detection kit (ZK-8005; ZSGB-Bio, Beijing, China) was used to determine the apoptosis rate in rat liver tissues. Five random fields in each section were evaluated by light microscopy (Olympus Optical Co. Ltd., Tokyo, Japan). Apoptotic cells were brown or brownish in color and with apoptotic cell morphology. Apoptosis was reported as the apoptosis index, and apoptosis (%)=(TUNEL-positive cells/total cells)×100.

Measurement of malondialdehyde (MDA), glutathione (GSH), superoxide dismutase (SOD) levels

Assay kits were used to determine MDA, SOD (Abcam), and GSH (Sigma-Aldrich) levels in cultured cells and liver tissues following manufacturer's instructions.

RNA immunoprecipitation (RIP)

Magna RIP RNA-binding protein immunoprecipitation kits (Millipore Corp, Billerica, MA, USA) was used for the RIP as-

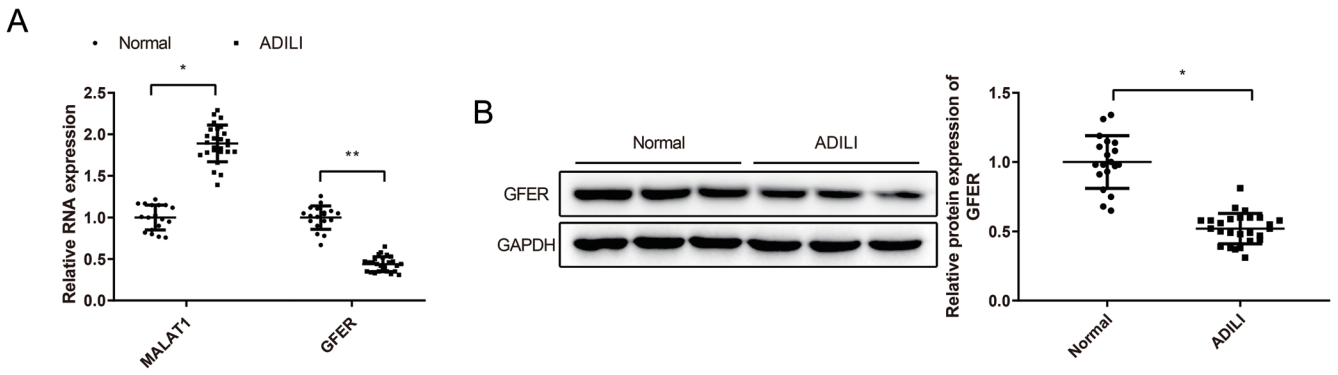

Fig. 1. Elevated MALAT1 expression and reduced GFER in ALI. Expression of MALAT1 and GFER in serum by qRT-PCR (A) and western blotting (B). *p<0.05, **p<0.01 vs. normal group, n=19/26. ALI, acute liver injury.

say. Briefly, HL7702 cells were lysed in 100 μL lysis buffer containing protease and RNase inhibitors, and then the protein lysate was incubated with rabbit anti-human EZH2 antibody (ab186006 1:500; Abcam) at 4°C for 30 m or anti-IgG antibody (ab109489, 1:100; Abcam) as the control. Subsequently, 10–50 μL of protein A/G beads were added and incubated with the cells at 4°C overnight. After incubation, the protein A/G-bead-antibody complexes were washed 3–4 times in 1 mL lysis buffer, and RNA was extracted and purified using the RNA extraction method. qRT-PCR was carried out with a MALAT1-specific primer to identify the interaction between EZH2 and MALAT1.

Chromatin immunoprecipitation (ChIP)

The ChIP assay was performed with SimpleChIP Plus sonication chromatin IP kits following the manufacturer's (Cell Signaling Technology) instructions. HL7702 cells were fixed in 1% formalin to crosslink DNA and proteins. Then, the cells were lysed in lysis buffer and nuclear lysis buffer and ultrasonicated to generate 200–300 bp chromatin segments. The cell lysate was immunoprecipitated with protein A-beads conjugated with the corresponding antibodies, including anti-EZH2 antibody (ab228697; Abcam) and anti-histone 3 antibody (trimethyl-K27, ab6002; Abcam). Anti-IgG antibody (ab171870; Abcam) was added as a negative control. Protein-DNA crosslinking was reversed the RNA was purified, and enrichment of the DNA segment was detected by qRT-PCR.

Hematoxylin and eosin (H&E) staining

Rat liver tissues were collected, fixed in 10% neutral buffered formalin (Beijing Solarbio Science & Technology Co., Ltd.) for 24 h, dehydrated, embedded in paraffin, cut into 4 μm serial sections, and stained with H&E (Beijing Solarbio Science & Technology Co., Ltd.). Tissue histology was evaluated by optical microscopy (Olympus Optical, Tokyo, Japan).

Immunohistochemistry

Collected liver tissues were fixed in 4% paraformaldehyde for 48 h, embedded in paraffin, and sectioned at 4 μm. The sections were baked for 20 m, dewaxed in xylene, and washed once in distilled water. After washing three times in PBS, the sections were placed in 3% H_2O_2 for 10 m and subjected to antigen retrieval. After washing with PBS three times, the sections were blocked in goat serum at room temperature for 20 m. Excess serum was discarded, and the primary antibody against Ki-67 (ab16667, 1:200; Abcam) was added to the sections for incubation (4°C, overnight). Afterwards, the sections were incubated with secondary antibody at room temperature for 1 h and washed three times in PBS. Color development was sustained for 1–3 m using diaminobenzidine solution, and H&E was then used for 3 m for nuclear staining. The sections were then dehydrated, permeabilized, and cover slipped for observation. The percentage of positive cells in five randomly selected fields was reported (positive cells (%)=(positive cells/total cells)×100.

Statistical analysis

GraphPad 7.0 software was used for the statistical analysis, and data were reported as means ± SD. The significance of between-group differences was determined by *t*-tests. Multiple comparisons was carried out with one-way analysis of variance followed by Tukey's multiple comparisons test. *P*-values <0.05 were considered statistically significant.

Results

MALAT1 was upregulated and GFER downregulated in ALI

To explore the expression of MALAT1 and GFER in patients with ALI, we included 26 patients with ADILI and 19 healthy individuals. There were no significant differences in sex or age between the two groups. Compared with the normal group, the serum levels of ALT, AST, γ-GT, alkaline phosphatase (ALP), and TBil, and the RUCAM scores of patients in the ADILI group increased significantly (Table 2; p<0.05). The results of qRT-PCR and western blotting showed that, compared with the normal group, the expression of MALAT1 in the serum of patients in the ADILI group increased, and the expression of GFER decreased (Fig. 1A, B; p<0.05). The results indicated that MALAT1 was highly expressed but GFER was weakly expressed in the serum of patients with ALI.

MALAT1 was upregulated and GFER downregulated in LPS-induced HL7702 cells

Human hepatocytes HL7702 were treated with LPS to induce an ALI cellular model, and ALT, AST, and LDH levels were assayed in the culture supernatant. LPS induction

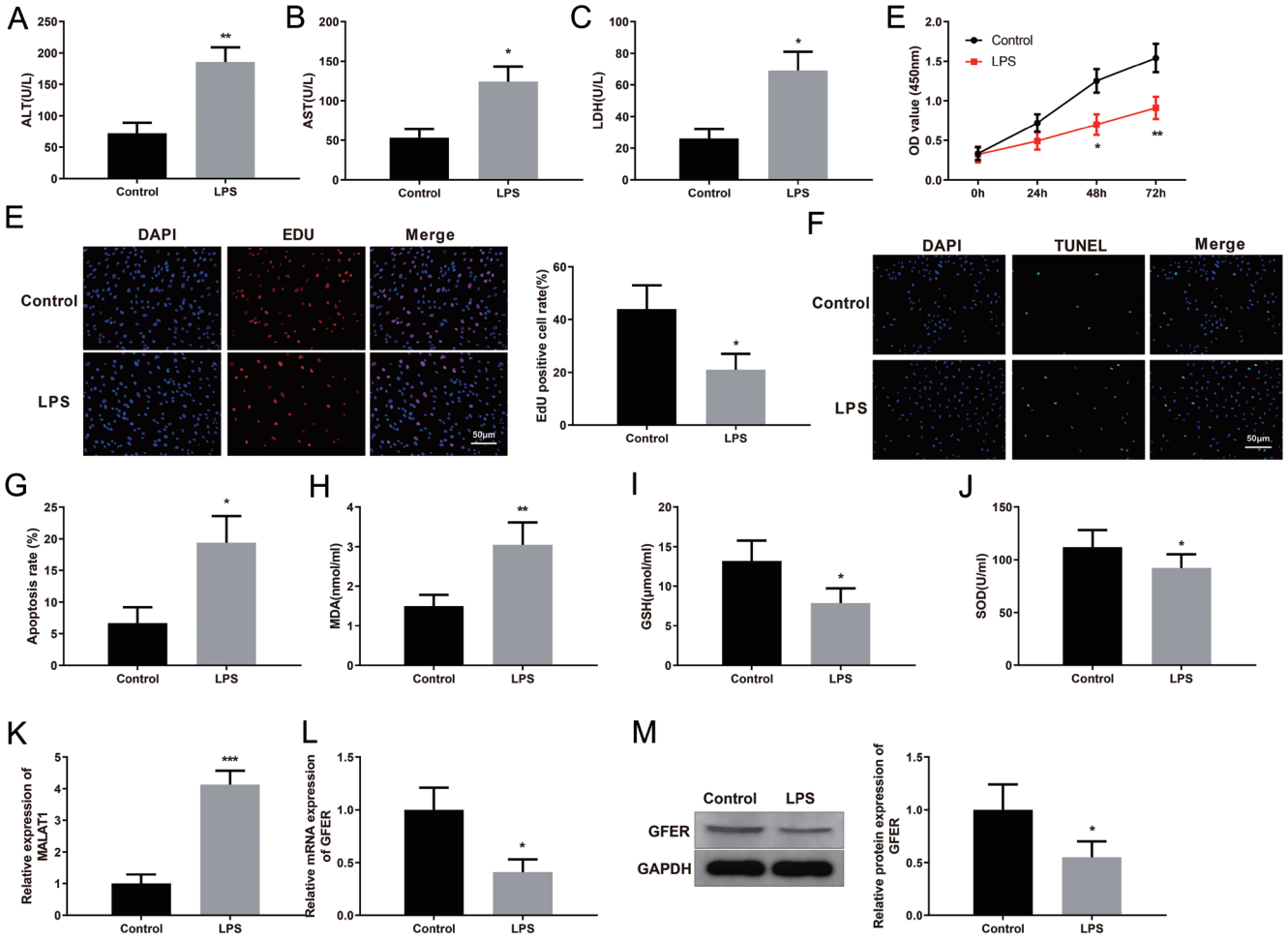

Fig. 2. MALAT1 expression was increased, and GFER expression was reduced, in LPS-induced HL7702 cells. After the ALI model was induced in HL7702 cells LPS, factors reflecting liver function, ALT (A), AST (B) and LDH (C) were assayed; cell proliferation was determined by CCK-8 assay (D) and EdU staining (E); TUNEL staining was used to assay cell apoptosis (F, G); MDA (H), GSH (I), and SOD (J) were assayed in cells. MALAT1 expression in HL7702 cells was assayed by qRT-PCR (K); mRNA and protein expression of GFER were assayed by qRT-PCR (L) and western blotting (M). *p<0.05, **p<0.01, ***p<0.001 vs. the control group. n=3. ALI, acute liver injury; ALT, alanine aminotransferase; AST, aspartic transaminase; GSH, glutathione; LDH, lactic dehydrogenase; LPS, lipopolysaccharide; MDA, malondialdehyde; SOD, superoxide dismutase.

increased ALT, AST, and LDH levels (Fig. 2A, C; p<0.05). The CCK-8 assay found that proliferation was decreased in the LPS group compared with the control group (Fig. 2D; p<0.05), which was confirmed by EdU staining (Fig. 2E; p<0.05). TUNEL staining found that the cell apoptosis rate was increased in the LPS group compared with the control group (Fig. 2F, G; p<0.05). Assays of MDA, SOD, and GSH in cells found that after LPS treatment, MDA increased significantly and SOD and GSH decreased significantly (Fig. 2H, J; p<0.01). Moreover, qRT-PCR and western blot assays found that LPS increased MALAT1 expression (Fig. 2K; p<0.001) and decreased GFER expression (Fig. 2L, M; p<0.05) in HL7702 cells compared with the control group. Overall, LPS induction enhanced MALAT1 expression and reduced GFER expression in HL7702 cells.

Downregulation of MALAT1 suppressed cell apoptosis and oxidative stress injury but induced cell proliferation through GFER

HL7702 cells were transfected with sh-MALAT1, oe-MALAT1, sh-GFER, or oe-GFER for 24 h, followed by treatment with LPS for 16 h. The transfection efficiency was validated by qRT-PCR and western blot analysis (Fig. 3A–D; p<0.05). In addition, MALAT1 overexpression inhibited GFER expression and MALAT1 knockdown enhanced GFER expression (Fig. 3B–D; p<0.05). However, overexpression or knockdown of GFER did not influence MALAT1 expression (Fig. 3A). Introduction of MALAT1 overexpression or GFER knockdown substantially increased the levels of ALT, AST and LDH, while MALAT1 knockdown or GFER overexpression had the opposite effects (Fig. 3E–G; p<0.05). Compared with the LPS + oe-MALAT1 group, the LPS + oe-MALAT1 + oe-GFER group had decreased ALT, AST and LDH levels (Fig. 3E–G; p<0.05). Moreover, MALAT1 overexpression or GFER knockdown inhibited HL7702 cell proliferation and induced cell apoptosis and oxidative stress injury, but MALAT1 knockdown or GFER overexpression increased the proliferation rate and decreased the apoptosis rate and oxidative stress injury (Fig. 3H–M; p<0.05). In the LPS + oe-MALAT1 + oe-GFER group, HL7702 cells possessed increased proliferative ability and decreased apoptosis rate and oxidative stress injury than those in the LPS + oe-MALAT1 group (Fig. 3H–M; p<0.05). The data indicate that downregulation of MALAT1

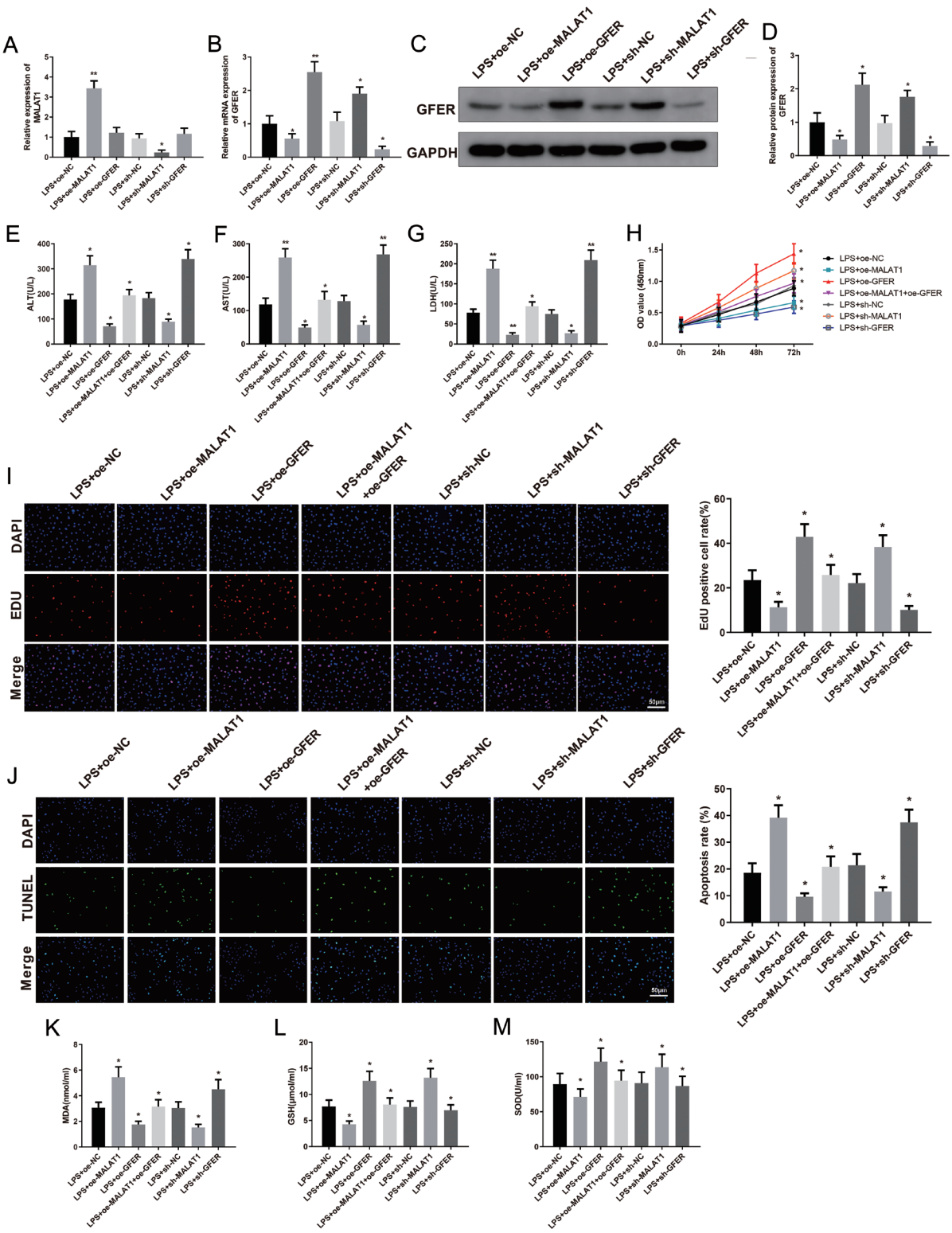

Fig. 3. Decreased MALAT1 suppresses hepatocyte apoptosis and oxidative stress injury and induces proliferation by regulation of GFER. HL7792 cells were transfected or co-transfected with sh-MALAT1, oe-MALAT1, sh-GFER and oe-GFER for 24 h, followed by LPS treatment. MALAT1 expression was assayed by qRT-PCR (A); GFER expression was assayed by qRT-PCR (B) and western blotting (C, D); ALT (E), AST (F) and LDH (G) were assayed in HL7702 cells; cell proliferation measured by CCK-8 assays (H) and EdU staining (I); Apoptosis of HL7702 cells was assayed by TUNEL staining (J); MDA (K), GSH (L), and SOD (M) levels in cells. *p<0.05, **p<0.01 vs. the LPS + oe-NC, LPS + sh-NC, or LPS + oe-MALAT1 group. n=3. ALT, alanine aminotransferase; AST, aspartic transaminase; LDH, lactic dehydrogenase; MDA, malondialdehyde; GSH, glutathione; NC, negative control; SOD, superoxide dismutase.

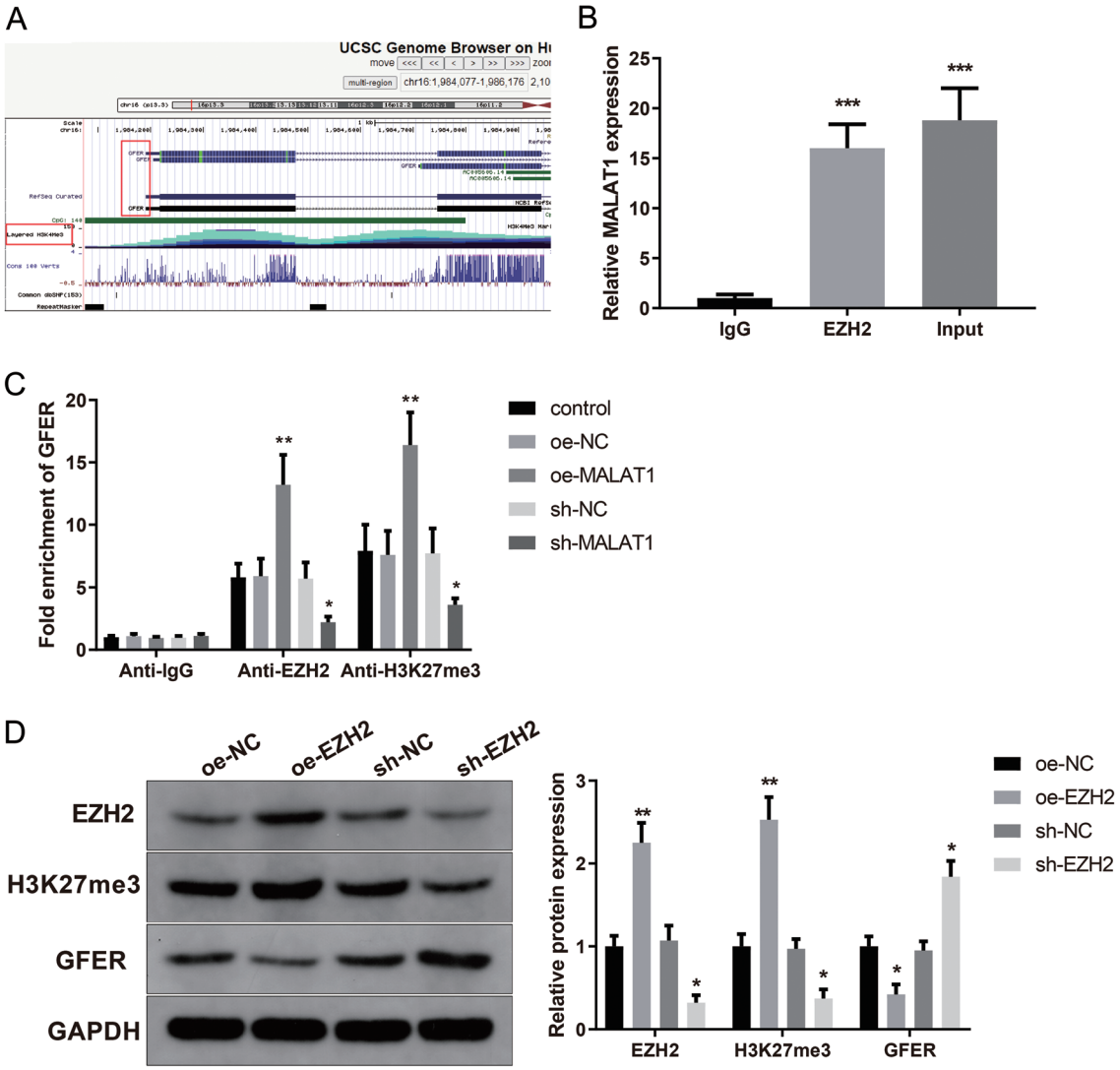

Fig. 4. MALAT1 suppresses GFER expression through recruiting EZH2 to the GFER promoter region. The H3K27me3 methylation peak in the GFER promoter region was predicted by the UCSU database (A); RIP assays was performed to identify the interaction between MALAT1 and EZH2 (B), ***p<0.001 vs. the IgG group; ChIP-PCR was used to detect the enrichment of EZH2 and H3H27me3 expression in the GFER promoter region (C), *p<0.05, **p<0.01 vs. the oe-NC or sh-NC group; After transfection of oe-EZH2 or sh-EZH2 into HL7702 cells, western blotting quantified EZH2, H3K27me3 and GFER expression (D), *p<0.05, **p<0.01 vs. the oe-NC or sh-NC group. n=3. ChIP, chromatin immunoprecipitation; NC, negative control; RIP, RNA immunoprecipitation.

inhibited hepatocyte apoptosis and oxidative stress injury but promoted cell proliferation by regulating GFER.

MALAT1 recruited EZH2 to the GFER promoter region to inhibit GFER expression

GFER significantly reduced ALT and AST in a mouse ALI model, and alleviated liver injury caused by ischemia-reperfusion.[20,21] The University of California Santa Cruz (UCSU) genome browser (http://genome-asia.ucsc.edu/) predicted the presence of H3K27me3 methylation peak in the GFER promoter region (Fig. 4A). Inhibition of MALAT1 reduces liver ischemia-reperfusion injury,[11] and MALAT1 changes the progression of liver fibrosis by regulating SIRT1.[22] A previous study reported that MALAT1 recruited histone methyltransferase EZH2 to the pri-miR-22 promoter region to inhibit miR-22 expression.[13] In this study, MALAT1 expression was negatively associated with GFER expression in the cellular ALI model, and the regulation of HL7702 cell proliferation and apoptosis by MALAT1 was involved in GFER. We hypothesized that MALAT1 recruited EZH2 to the GFER promoter region to suppress GFER expression. As expected, the RIP assay identified the interaction between MALAT1 and EZH2 (Fig. 4B; p<0.001). A ChIP assay was performed to confirm whether EZH2 regulated GFER expression via H2K27me3 methylation. EZH2 and H3K27me3 were found to be more abundant in the GFER promoter region in the oe-MALAT1 group than in the oe-NC group (p<0.01); enrichment of EZH2 and H3K27me3 in the GFER promoter region was reduced in the sh-MALAT1 group when compared with the sh-NC group (Fig. 4C; p<0.05). HL7702 cells were transfected with oe-EZH2 or sh-EZH2, and western blots of EZH2 expression demonstrated that transfection of oe-EZH2 promoted EZH2 and H3K27me3 expression and reduced GFER expression. sh-EZH2 treatment resulted in contrary findings

(Fig. 4D; $p<0.05$). Overall, the results show that MALAT1 inhibited GFER expression by recruiting EZH2 to the GFER promoter region and promoting H3K27me3 methylation.

MALAT1/EZH2/GFER activated the AMPK/mTOR signaling pathway

HL7702 cells were transfected with sh-MALAT1, oe-MALAT1, sh-EZH2, oe-EZH2, sh-GFER and oe-GFER for 24 h, followed by treatment with LPS for 16 h. The levels of phosphorylated proteins active in the AMPK/mTOR signaling pathway were assayed by western blotting. MALAT1/EZH2 overexpression or GFER knockdown significantly upregulated phosphorylated AMPK levels and downregulated phosphorylated mTOR levels in HL7702 cells;. MALAT1/EZH2 knockdown or GFER overexpression had the opposite effects (Fig. 5A–C; $p<0.05$).

After HL7702 cells were transfected with oe-MALAT1 lentiviral vector and its control (oe-NC) for 24 h, they were treated with the AMPK inhibitor Compound C (CC) for 1 h, induced by LPS for 16 h, and then collected for subsequent assays. Western blot assays demonstrated that compared with the LPS + oe-NC group, phosphorylated AMPK level was decreased and phosphorylated mTOR expression was increased in the LPS + oe-NC + CC group. HL7702 cells in the LPS + oe-MALAT1 group had the reverse responses; phosphorylated AMPK level was reduced and that of mTOR was increased in the LPS + oe-MALAT1 + CC group compared with the LPS + oe-MALAT1 group (Fig. 5D–F; $p<0.01$).

In the LPS + oe-NC + CC group, the levels of ALT, AST and LDH were decreased (Fig. 5G–I; $p<0.05$), HL7702 cell proliferation was increased (Fig. 5J, K; $p<0.05$), and the apoptosis rate and oxidative stress injury were inhibited (Fig. 5L–O; $p<0.05$) compared with those in the LPS + oe-NC group. HL7702 cells in the LPS + oe-MALAT1 group had increased ALT, AST, and LDH levels (Fig. 5G–I; $p<0.05$) concurrent with decreased cell proliferation (Fig. 5J, K; $p<0.05$) and enhanced apoptosis rate and oxidative stress injury (Fig. 5L–O; $p<0.05$), compared with those in the LPS + oe-NC group. In the LPS + oe-MALAT1 + CC group, the levels of ALT, AST and LDH in HL7702 cell supernatant were suppressed (Fig. 5G–I; $p<0.05$) along with increased proliferation (Fig. 5J, K; $p<0.05$) and reduced apoptosis rate and oxidative stress injury (Fig. 5L–O; $p<0.05$). The data indicate that MALAT1/EZH2/GFER activated the AMPK/mTOR signaling pathway.

Downregulation of MALAT1 restored GFER expression in rats with ALI

Rats were intravenously injected with sh-MALAT1 or oe-GFER in the tail vein for 42 h, followed by treatment of LPS to induce ALI. We demonstrated that the levels of ALT, AST and LDH in rat serum were increased in the LPS group ($p<0.01$, vs. the saline group), while those of the LPS + sh-MALAT1 group and the LPS + oe-GFER group were lower than those in the LPS + sh-NC group and the LPS + oe-NC group (Fig. 6A–C). As shown by H&E staining, rats in the normal group and the saline group had normal histology with clear hepatic lobules and regular hepatic sinusoids. In contrast, rats in the LPS group had significant liver injury, manifested as cellular edema, hematolysis, diffuse necrosis, and inflammatory cell infiltration (Fig. 6D). However, LPS-induced injury was alleviated in the liver tissues of rats in the LPS + sh-MALAT1 and LPS + oe-GFER groups (Fig. 6D).

qRT-PCR and western blotting revealed an increase in MALAT1 expression (Fig. 6E; $p<0.01$) and a decrease in GFER expression (Fig. 6F, G; $p<0.05$) in the LPS group compared with those in the saline group. In the LPS + sh-MALAT1 group, MALAT1 expression was significantly reduced (Fig. 6E; $p<0.01$) and GFER expression was upregulated (Fig. 6F, G, $p<0.05$) in liver tissues, compared with the LPS + sh-NC group. Moreover, increased GFER expression ($p<0.001$) and unchanged MALAT1 expression ($p > 0.05$) were found in the LPS + oe-GFER group compared with the LPS + oe-NC group (Fig. 6E–G). Taken together, downregulation of MALAT1 promoted GFER expression in ALI-model rats.

Downregulation of MALAT1 or overexpression of GFER inhibited ALI in vivo

Rats were injected with sh-MALAT1 or oe-GFER in the tail vein for 42 h, followed by LPS induction for modelling, and then immunohistochemistry was performed. Mice in the LPS group had fewer Ki-67-positive liver cells than the saline group, but MALAT1 knockdown or GFER overexpression increased the percentage of Ki-67-positive cells in liver tissues (Fig. 7A; $p<0.05$). In addition, TUNEL staining indicated increased apoptosis rate in rat liver tissue from the LPS group ($p<0.01$, vs. the saline group) and decreased hepatocyte apoptosis in the LPS + sh-MALAT1 or the LPS + oe-GFER group (both $p<0.05$) (Fig. 7B). We also found that MDA was increased and SOD and GSH were decreased in liver tissue from the LPS group relative to the saline group. In the LPS + sh-MALAT1 group or the LPS + oe-GFER group, MDA level was decreased and SOD and GSH levels were increased (Fig. 7C–E; $p<0.01$).

In addition, liver tissues in the LPS group were found to have upregulated levels of phosphorylated AMPK (Fig. 7F, G; $p<0.01$) and downregulated levels of phosphorylated mTOR (Fig. 7F. H; $p<0.05$). However, MALAT1 knockdown or GFER overexpression reduced phosphorylated AMPK and increased phosphorylated mTOR levels in liver tissue (Fig. 7F–H; $p<0.05$). Thus, these data proved the ameliorative effect of MALAT1 downregulation or GFER overexpression on ALI *in vivo*.

Discussion

ALI is a severe, acute disease with a high mortality. It is characterized by acute hepatocyte necrosis, and there have not been any treatment breakthroughs in the last few decades.[23,24] Recently, various lncRNAs, including DINO, NEAT1, and XIST, and their downstream genes have been investigated to explain the progression and improve the effectiveness of ALI treatment.[16,25,26] LPS, which was first found in the outer membrane of gram-negative bacteria, has been widely used *in vivo* and *in vitro* to mimic the pathology of ALI.[27–29] In this study, we successfully established cellular and animal models of ALI using LPS, and MALAT1 was found to inhibit cell proliferation and promote apoptosis in LPS-induced rats and hepatocytes. MALAT1 has been found to limit proliferation and induce apoptosis of human renal tubular epithelial cells in the presence of LPS,[30] and MALAT1 knockdown was found to block LPS-induced acute lung injury by inhibiting apoptosis and improving cell viability.[31] The apoptosis-promoting effect of MALAT1 has been previously reported in hepatocytes.[31] However, Li *et al*.[32] reported that MALAT1 overexpression was required for accelerating hepatocyte proliferation and liver regeneration. Our in vivo and *in vitro* experiments showed that MALAT1 was upregulated after LPS exposure and identified as an ALI-promoting gene. GFER, also known as ALR, protects against chemical- or toxin-related ALI,[33,34] ischemia reperfusion-induced liver and kidney injury.[35,36] Deletion of ALR accelerates steatohepatitis and hepatocellular carcinoma.[37] Therefore, we ex-

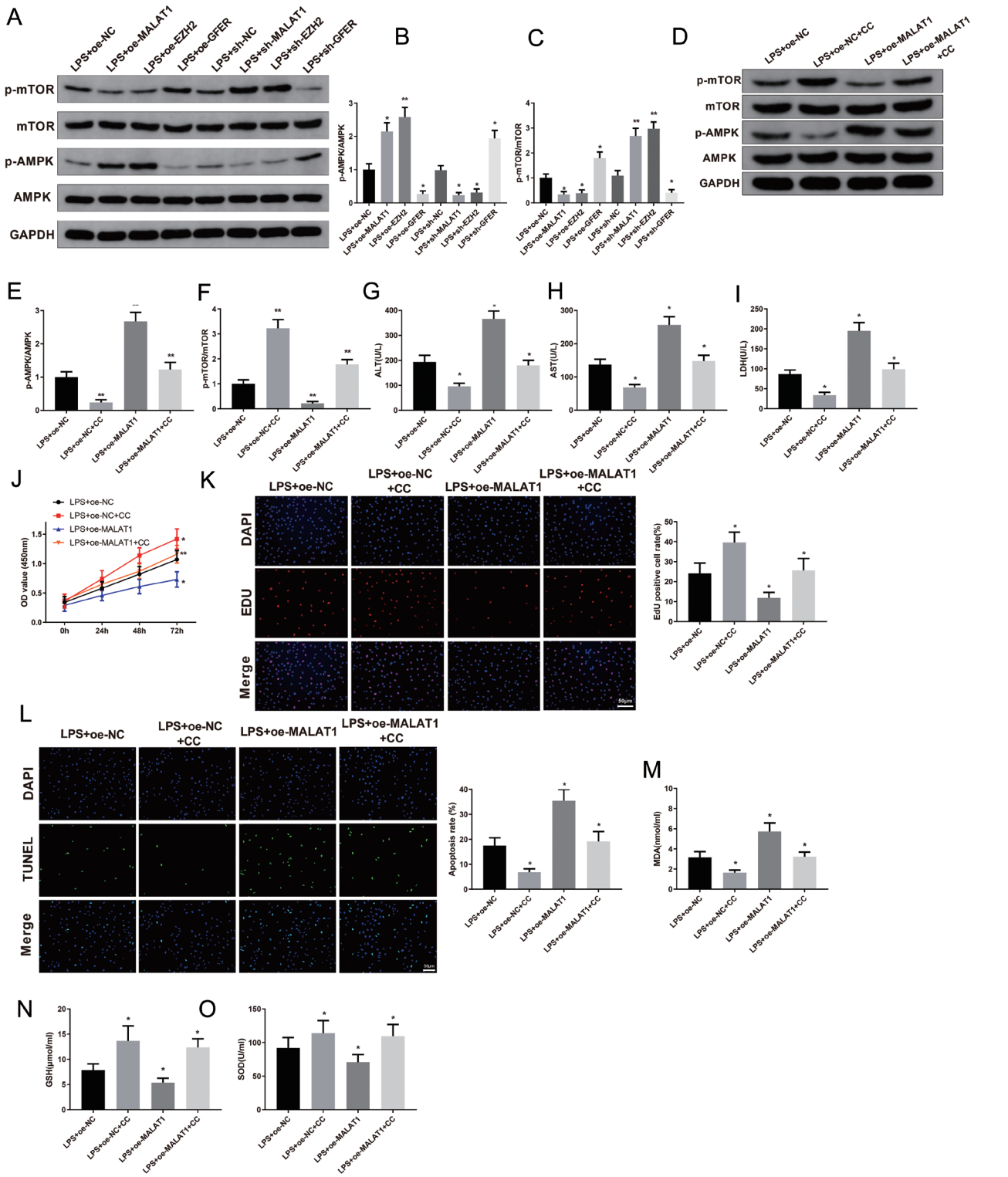

Fig. 5. MALAT1/EZH2/GFER activates the AMPK/mTOR signaling pathway. After introduction of sh-MALAT1, oe-MALAT1, sh-EZH2, oe-EZH2, sh-GFER, and oe-GFER for 24 h, HL7702 cells were subjected to LPS treatment for 16 h. Phosphorylated AMPK and mTOR were assayed by western blotting (A–C), *p<0.05, **p<0.01 vs. the LPS + oe-NC or LPS + sh-NC group. HL7702 cells were transfected with oe-MALAT1 or oe-NC for 24 h and then stimulated with the AMPK inhibitor Compound C for 1 h, and treated with LPS. Phosphorylated AMPK and mTOR levels were determined by Western blotting (D, F); ALT (G), AST (H) and LDH (I); Cell proliferation was determined by CCK-8 assays (J) and EdU staining (K); Cell apoptosis was assayed by TUNEL staining (L), Determination of MDA (M), GSH (N), and SOD (O) in cells. *p<0.05 vs. LPS + oe-NC or LPS + oe-MALAT1 group. n=3. AST, aspartic transaminase; ALT, alanine aminotransferase; GSH, glutathione; LDH, lactic dehydrogenase; LPS, lipopolysaccharide; MDA, malondialdehyde; NC, negative control; SOD, superoxide dismutase.

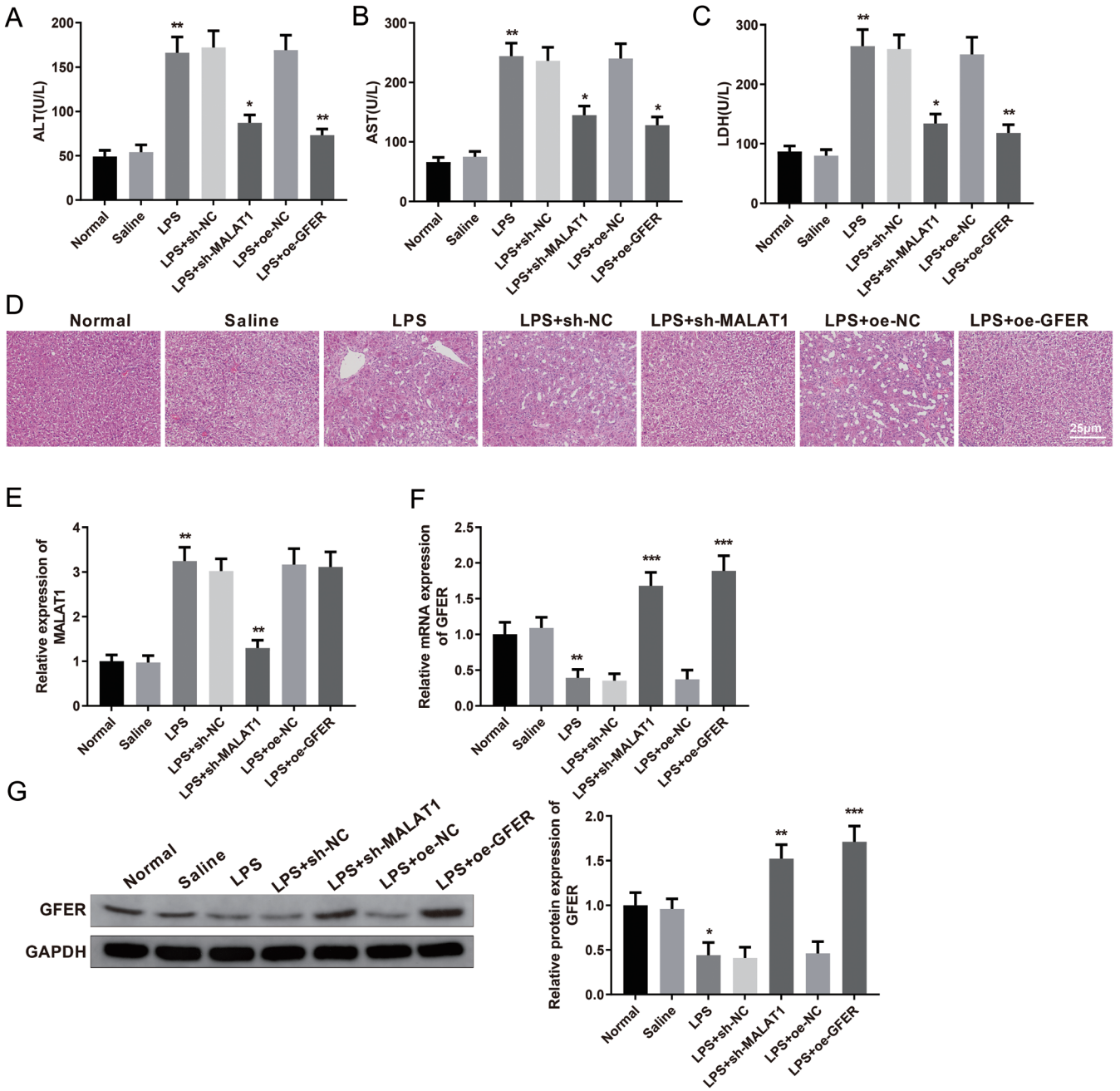

Fig. 6. Downregulation of MALAT1 increases GFER expression in ALI-treated rats. Following injection of sh-MALAT1/oe-GFER and LPS induction, ALT (A), AST (B) and LDH (C) were assayed in rat serum; Histology of representative rat liver liver tissue stained with hematoxylin and eosin (D); MALAT1 expression (E) and GFER expression (F) in liver tissue were assayed by qRT-PCR and western blotting (G). *p<0.05, **p<0.01, ***p<0.001 vs. the saline, LPS + sh-NC, or LPS + oe-NC group. n=6. ALI, acute liver injury; ALT, alanine aminotransferase; AST, aspartic transaminase; LDH, lactic dehydrogenase; LPS, lipopolysaccharide; NC, negative control.

amined the expression of GFER in LPS-induced hepatocytes, which showed a decrease in GFER expression. Overexpression of GFER alleviated hepatocyte apoptosis, excessive hepatocyte proliferation, and improved liver function after LPS insult. Intriguingly, MALAT1 was negatively associated with, and significantly regulated, GFER expression at the cellular and animal levels. In addition, the ALI-promoting effect of MALAT1 was offset by GFER upregulation, indicated by decreases in serum AST/ALT, hepatocyte apoptosis, and enhanced proliferation of hepatocytes. The results indicated that MALAT1 regulated GFER expression to aggravate ALI. We then focused on elucidating the mechanism of MALAT1 regulation of GFER in ALI.

MALAT1 has oncogenic activity through EZH2-mediated suppression of miR-217 expression in lung carcinogenesis.[38] In the presence of MALAT1, silencing of EZH2 has been shown to reduce apoptosis and enhance cardiac function.[13] Increased MALAT1 recruits EZH2 to its downstream gene to promote H3K27me3 expression for specific transcription inhibition.[39] EZH2 can modify the enrichment of its catalyzed

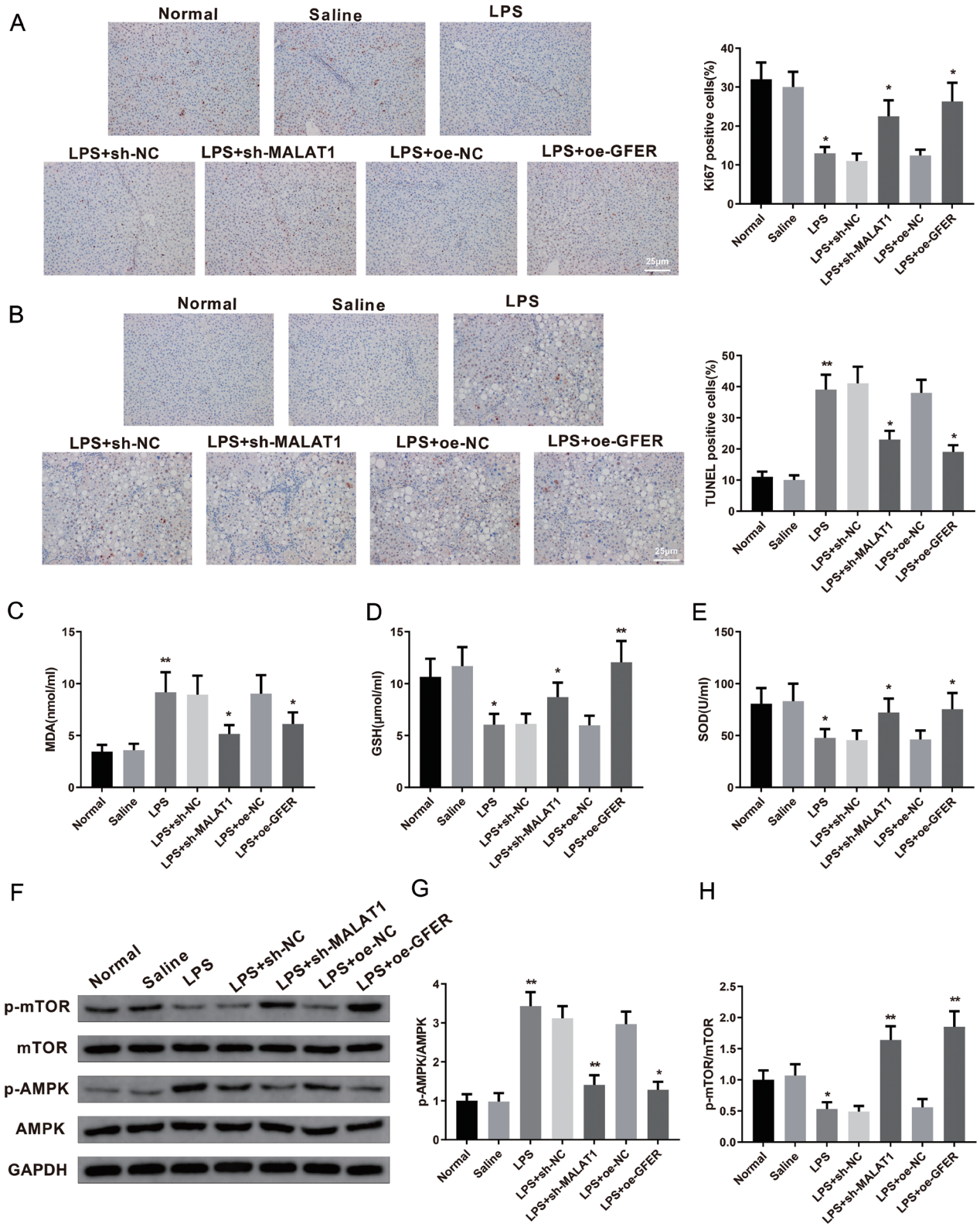

Fig. 7. Downregulation of MALAT1 or overexpression of GFER suppresses ALI *in vivo*. LPS induction was performed 42 h after injection of sh-MALAT1/oe-GFER. Immunohistochemical staining of Ki-67 in rat liver tissues (A); TUNEL staining of apoptotic cell in liver tissue (B); Determination of MDA (C), GSH (D), and SOD (E) levels in cells; and western blotting of phosphorylated AMPK and mTOR (F–H), *p<0.05, **p<0.01 vs. the saline, LPS + sh-NC or LPS + oe-NC group. n=6. ALI, acute liver injury; GSH, glutathione; MDA, malondialdehyde; NC, negative control; LPS, lipopolysaccharide; SOD, superoxide dismutase.

H3K27me3 and contribute to the pathogenesis of liver failure by triggering the release of tumor necrosis factor (TNF) and other pro-inflammatory cytokines.[40] Inhibition of EZH2 blunts H3K27me3 and restrains the activities of serum ALT and AST.[41] We predicted an H3K27me3 methylation peak in the GFER peak, indicating that MALAT1 might regulate GFER expression through methylation. Our functional experiments identified an interaction between MALAT1 and EZH2, and further demonstrated that MALAT1 overexpression significantly enhanced the enrichment of EZH2 and H3K27me3 in the GFER promoter region. The study firstly demonstrated that MALAT1 suppressed GFER expression by recruiting EZH2 to the GFER promoter region, enhancing H3K27me3 methylation, and aggravating ALI.

AMPK regulates energy homeostasis and metabolism, and mTOR is an enzyme downstream of AMPK.[42] Activation of the AMPK/mTOR signaling pathway has been shown to be involved in liver diseases, including nonalcoholic fatty liver disease and ALI.[43–45] More important, Pu *et al*.[46] found that deletion of ALR induced increased AMPK phosphorylation and decreased mTORC1 phosphorylation, and increased both autophagy flux and apoptosis. In this study, phosphorylated AMPK was increased, and phosphorylated mTOR was reduced in ALI model rats. At the same time, MALAT1 inhibition or GFER overexpression decreased the expression of p-AMPK and promoted p-mTOR expression. Inhibiting the phosphorylation of AMPK by Compound C inhibited ALT, AST, and LDH, and hepatocyte apoptosis, and improved hepatocyte proliferation. Knockdown of MALAT1 or overexpression of GFER had a similar effect to that of Compound C in ALI. The AMPK/mTOR pathway is a typical regulator of autophagy.[47] Both endogenous and exogenous interleukin-37 protect against ischemia reperfusion-induced hepatic injury by restraining excessive autophagy and apoptosis by regulating the AMPK/mTOR signaling pathway.[48] Therefore, much attention should be paid in future studies to whether MALAT1/EZH2/GFER participates in ALI by activating the AMPK/mTOR pathway to affect hepatocyte autophagy.

This study revealed that MALAT1 upregulation was associated with decreased proliferation, enhanced apoptosis, and aggravation of liver injury, which sheds light on the prevention and treatment of ALI. Notably, we showed that MALAT1 inhibited GFER by recruiting EZH2 to the GFER promoter region and enhancing H3K27me3 methylation, thus resulting in deterioration of ALI. Activation of the AMPK/mTOR signaling pathway was also linked to the ALI-promoting effect of MALAT1. The study thus characterized a possible regulatory mechanism of MALAT1 exacerbating ALI, which contributes to understanding ALI progression and provides a novel approach for ALI treatment. Further studies are required to explain the regulation and methylation of the molecules by MALAT1 in ALI to boost the application of their therapeutic benefits in clinical practice.

Funding

None to declare.

Conflict of interest

The authors have no conflict of interests related to this publication.

Author contributions

Conceived the study (LC), designed the experiments (XK), performed the experiments (LC), analyzed the data (XK), provided critical materials (XM, LH, YD), wrote the manuscript (YZ), and supervised the study (CL). All the authors have read and approved the final version for publication.

Data sharing statement

The datasets used or analyzed during the current study are available from the corresponding author on reasonable request.

References

[1] Kim JW, Yang D, Jeong H, Park IS, Lee MH, Lim CW, *et al*. Dietary zerumbone, a sesquiterpene, ameliorates hepatotoxin-mediated acute and chronic liver injury in mice. Phytother Res 2019;33(5):1538–1550. doi:10.1002/ptr.6346, PMID:30868670.
[2] Zheng Y, Cui B, Sun W, Wang S, Huang X, Gao H, *et al*. Potential Crosstalk between Liver and Extra-liver Organs in Mouse Models of Acute Liver Injury. Int J Biol Sci 2020;16(7):1166–1179. doi:10.7150/ijbs.41293, PMID:32174792.
[3] Breu AC, Patwardhan VR, Nayor J, Ringwala JN, Devore ZG, Ganatra RB, *et al*. A Multicenter Study Into Causes of Severe Acute Liver Injury. Clin Gastroenterol Hepatol 2019;17(6):1201–1203. doi:10.1016/j.cgh.2018.08.016, PMID:30103039.
[4] McGovern AJ, Vitkovitsky IV, Jones DL, Mullins ME. Can AST/ALT ratio indicate recovery after acute paracetamol poisoning? Clin Toxicol (Phila) 2015;53(3):164–167. doi:10.3109/15563650.2015.1006399, PMID:25652258.
[5] Li M, Zhao H, Wu J, Wang L, Wang J, Lv K, *et al*. Nobiletin Protects against Acute Liver Injury via Targeting c-Jun N-Terminal Kinase (JNK)-Induced Apoptosis of Hepatocytes. J Agric Food Chem 2020;68(27):7112–7120. doi:10.1021/acs.jafc.0c01722, PMID:32538091.
[6] Karvellas CJ, Subramanian RM. Current Evidence for Extracorporeal Liver Support Systems in Acute Liver Failure and Acute-on-Chronic Liver Failure. Crit Care Clin 2016;32(3):439–451. doi:10.1016/j.ccc.2016.03.003, PMID:27339682.
[7] Sugawara K, Nakayama N, Mochida S. Acute liver failure in Japan: definition, classification, and prediction of the outcome. J Gastroenterol 2012;47(8):849–861. doi:10.1007/s00535-012-0624-x, PMID:22825549.
[8] Shi X, Jiang X, Yuan B, Liu T, Tang Y, Che Y, *et al*. LINC01093 Upregulation Protects against Alcoholic Hepatitis through Inhibition of NF-κB Signaling Pathway. Mol Ther Nucleic Acids 2019;17:791–803. doi:10.1016/j.omtn.2019.06.018, PMID:31450097.
[9] Takahashi K, Yan I, Haga H, Patel T. Long noncoding RNA in liver diseases. Hepatology 2014;60(2):744–753. doi:10.1002/hep.27043, PMID:24493213.
[10] Ma T, Jia H, Ji P, He Y, Chen L. Identification of the candidate lncRNA biomarkers for acute kidney injury: a systematic review and meta-analysis. Expert Rev Mol Diagn 2021;21(1):77–89. doi:10.1080/14737159.2021.1873131, PMID:33612038.
[11] Zhang Y, Zhang H, Zhang Z, Li S, Jiang W, Li X, *et al*. LncRNA MALAT1 cessation antagonizes hypoxia/reoxygenation injury in hepatocytes by inhibiting apoptosis and inflammation via the HMGB1-TLR4 axis. Mol Immunol 2019;112:22–29. doi:10.1016/j.molimm.2019.04.015, PMID:31075559.
[12] Liu Y, Wang X, Li P, Zhao Y, Yang L, Yu W, *et al*. Targeting MALAT1 and miRNA-181a-5p for the intervention of acute lung injury/acute respiratory distress syndrome. Respir Res 2021;22(1):1. doi:10.1186/s12931-020-01578-8, PMID:33407436.
[13] Wang C, Liu G, Yang H, Guo S, Wang H, Dong Z, *et al*. MALAT1-mediated recruitment of the histone methyltransferase EZH2 to the microRNA-22 promoter leads to cardiomyocyte apoptosis in diabetic cardiomyopathy. Sci Total Environ 2021;766:142191. doi:10.1016/j.scitotenv.2020.142191, PMID:33097254.
[14] Lin N, Yao Z, Xu M, Chen J, Lu Y, Yuan L, *et al*. Long noncoding RNA MALAT1 potentiates growth and inhibits senescence by antagonizing ABI3BP in gallbladder cancer cells. J Exp Clin Cancer Res 2019;38(1):244. doi:10.1186/s13046-019-1237-5, PMID:31174563.
[15] Huang H, Li H, Chen X, Yang Y, Li X, Li W, *et al*. HMGA2, a driver of inflammation, is associated with hypermethylation in acute liver injury. Toxicol Appl Pharmacol 2017;328:34–45. doi:10.1016/j.taap.2017.05.005, PMID:28502886.
[16] Wang Q, Liu L, Zhang S, Ming Y, Liu S, Cheng K, *et al*. Long noncoding RNA NEAT1 suppresses hepatocyte proliferation in fulminant hepatic failure through increased recruitment of EZH2 to the LATS2 promoter region and promotion of H3K27me3 methylation. Exp Mol Med 2020;52(3):461–472. doi:10.1038/s12276-020-0387-z, PMID:32157157.
[17] Ibrahim S, Weiss TS. Augmenter of liver regeneration: Essential for growth and beyond. Cytokine Growth Factor Rev 2019;45:65–80. doi:10.1016/j.cytogfr.2018.12.003, PMID:30579845.
[18] Francavilla A, Pesetti B, Barone M, Morgano A, Bovenga F, Napoli A, *et al*. Transient GFER knockdown in vivo impairs liver regeneration after partial hepatectomy. Int J Biochem Cell Biol 2014;53:343–351. doi:10.1016/j.biocel.2014.05.029, PMID:24880092.
[19] Danan G, Teschke R. RUCAM in Drug and Herb Induced Liver Injury:

The Update. Int J Mol Sci 2015;17(1):E14. doi:10.3390/ijms17010014, PMID:26712744.
[20] Dong Y, Kong W, An W. Downregulation of augmenter of liver regeneration impairs the therapeutic efficacy of liver epithelial progenitor cells against acute liver injury by enhancing mitochondrial fission. Stem Cells 2021;39(11):1546–1562. doi:10.1002/stem.3439, PMID:34310799.
[21] Kong WN, Li W, Bai C, Dong Y, Wu Y, An W. Augmenter of liver regeneration-mediated mitophagy protects against hepatic ischemia/reperfusion injury. Am J Transplant 2022;22(1):130–143. doi:10.1111/ajt.16757, PMID:34242470.
[22] Wu Y, Liu X, Zhou Q, Huang C, Meng X, Xu F, *et al*. Silent information regulator 1 (SIRT1) ameliorates liver fibrosis via promoting activated stellate cell apoptosis and reversion. Toxicol Appl Pharmacol 2015;289(2):163–176. doi:10.1016/j.taap.2015.09.028, PMID:26435214.
[23] Huang ZB, Zheng YX, Li N, Cai SL, Huang Y, Wang J, *et al*. Protective effects of specific cannabinoid receptor 2 agonist GW405833 on concanavalin A-induced acute liver injury in mice. Acta Pharmacol Sin 2019;40(11):1404–1411. doi:10.1038/s41401-019-0213-0, PMID:30918343.
[24] Wang H, Zhang H, Wang Y, Yang L, Wang D. Embelin can protect mice from thioacetamide-induced acute liver injury. Biomed Pharmacother 2019;118:109360. doi:10.1016/j.biopha.2019.109360, PMID:31545222.
[25] Khanal T, Leung YK, Jiang W, Timchenko N, Ho SM, Kim K. NR2E3 is a key component in p53 activation by regulating a long noncoding RNA DINO in acute liver injuries. FASEB J 2019;33(7):8335–8348. doi:10.1096/fj.201801881RR, PMID:30991008.
[26] Shen C, Li J. LncRNA XIST silencing protects against sepsis-induced acute liver injury via inhibition of BRD4 expression. Inflammation 2021;44(1):194–205. doi:10.1007/s10753-020-01321-x, PMID:32812145.
[27] Huynh DTN, Baek N, Sim S, Myung CS, Heo KS. Minor Ginsenoside Rg2 and Rh1 Attenuates LPS-Induced Acute Liver and Kidney Damages via Downregulating Activation of TLR4-STAT1 and Inflammatory Cytokine Production in Macrophages. Int J Mol Sci 2020;21(18):E6656. doi:10.3390/ijms21186656, PMID:32932915.
[28] Jayakumar T, Huang HC, Hsia CW, Fong TH, Khamrang T, Velusamy M, *et al*. Ruthenium derivatives attenuate LPS-induced inflammatory responses and liver injury via suppressing NF-κB signaling and free radical production. Bioorg Chem 2020;96:103639. doi:10.1016/j.bioorg.2020.103639, PMID:32036165.
[29] Li M, Wang S, Li X, Jiang L, Wang X, Kou R, *et al*. Diallyl sulfide protects against lipopolysaccharide/d-galactosamine-induced acute liver injury by inhibiting oxidative stress, inflammation and apoptosis in mice. Food Chem Toxicol 2018;120:500–509. doi:10.1016/j.fct.2018.07.053, PMID:30075314.
[30] Xu L, Hu G, Xing P, Zhou M, Wang D. Paclitaxel alleviates the sepsis-induced acute kidney injury via lnc-MALAT1/miR-370-3p/HMGB1 axis. Life Sci 2020;262:118505. doi:10.1016/j.lfs.2020.118505, PMID:32998017.
[31] Nan CC, Zhang N, Cheung KCP, Zhang HD, Li W, Hong CY, *et al*. Knockdown of lncRNA MALAT1 Alleviates LPS-Induced Acute Lung Injury via Inhibiting Apoptosis Through the miR-194-5p/FOXP2 Axis. Front Cell Dev Biol 2020;8:586869. doi:10.3389/fcell.2020.586869, PMID:33117815.
[32] Li C, Chang L, Chen Z, Liu Z, Wang Y, Ye Q. The role of lncRNA MALAT1 in the regulation of hepatocyte proliferation during liver regeneration. Int J Mol Med 2017;39(2):347–356. doi:10.3892/ijmm.2017.2854, PMID:28075444.
[33] Hu T, Sun H, Deng WY, Huang WQ, Liu Q. Augmenter of Liver Regeneration Protects Against Acetaminophen-Induced Acute Liver Injury in Mice by Promoting Autophagy. Shock 2019;52(2):274–283. doi:10.1097/SHK.0000000000001250, PMID:30138299.
[34] Liu L, Xie P, Li W, Wu Y, An W. Augmenter of Liver Regeneration Protects against Ethanol-Induced Acute Liver Injury by Promoting Autophagy. Am J Pathol 2019;189(3):552–567. doi:10.1016/j.ajpath.2018.11.006, PMID:30553838.
[35] Huang LL, Liao XH, Sun H, Jiang X, Liu Q, Zhang L. Augmenter of liver regeneration protects the kidney from ischaemia-reperfusion injury in ferroptosis. J Cell Mol Med 2019;23(6):4153–4164. doi:10.1111/jcmm.14302, PMID:30993878.
[36] Weiss TS, Lupke M, Dayoub R, Geissler EK, Schlitt HJ, Melter M, *et al*. Augmenter of Liver Regeneration Reduces Ischemia Reperfusion Injury by Less Chemokine Expression, Gr-1 Infiltration and Oxidative Stress. Cells 2019;8(11):E1421. doi:10.3390/cells8111421, PMID:31718093.
[37] Gandhi CR, Chaillet JR, Nalesnik MA, Kumar S, Dangi A, Demetris AJ, *et al*. Liver-specific deletion of augmenter of liver regeneration accelerates development of steatohepatitis and hepatocellular carcinoma in mice. Gastroenterology 2015;148(2):379–391.e4. doi:10.1053/j.gastro.2014.10.008, PMID:25448926.
[38] Lu L, Luo F, Liu Y, Liu X, Shi L, Lu X, *et al*. Posttranscriptional silencing of the lncRNA MALAT1 by miR-217 inhibits the epithelial-mesenchymal transition via enhancer of zeste homolog 2 in the malignant transformation of HBE cells induced by cigarette smoke extract. Toxicol Appl Pharmacol 2015;289(2):276–285. doi:10.1016/j.taap.2015.09.016, PMID:26415832.
[39] Hu H, Wu J, Yu X, Zhou J, Yu H, Ma L. Long non-coding RNA MALAT1 enhances the apoptosis of cardiomyocytes through autophagy inhibition by regulating TSC2-mTOR signaling. Biol Res 2019;52(1):58. doi:10.1186/s40659-019-0265-0, PMID:31783925.
[40] Zhou T, Sun Y, Li M, Ding Y, Yin R, Li Z, *et al*. Enhancer of zeste homolog 2-catalysed H3K27 trimethylation plays a key role in acute-on-chronic liver failure via TNF-mediated pathway. Cell Death Dis 2018;9(6):590. doi:10.1038/s41419-018-0670-2, PMID:29789597.
[41] Jiang Y, Xiang C, Zhong F, Zhang Y, Wang L, Zhao Y, *et al*. Histone H3K27 methyltransferase EZH2 and demethylase JMJD3 regulate hepatic stellate cells activation and liver fibrosis. Theranostics 2021;11(1):361–378. doi:10.7150/thno.46360, PMID:33391480.
[42] Liu LJ, Xu M, Zhu J, Li N, Zhao XZ, Gao HM. Adiponectin alleviates liver injury in sepsis rats through AMPK/MTOR pathway. Eur Rev Med Pharmacol Sci 2020;24(20):10745–10752. doi:10.26355/eurrev_202010_23435, PMID:33155235.
[43] Lu W, Mei J, Yang J, Wu Z, Liu J, Miao P, *et al*. ApoE deficiency promotes non-alcoholic fatty liver disease in mice via impeding AMPK/mTOR mediated autophagy. Life Sci 2020;252:117601. doi:10.1016/j.lfs.2020.117601, PMID:32304762.
[44] Wang Q, Wei S, Zhou S, Qiu J, Shi C, Liu R, *et al*. Hyperglycemia aggravates acute liver injury by promoting liver-resident macrophage NLRP3 inflammasome activation via the inhibition of AMPK/mTOR-mediated autophagy induction. Immunol Cell Biol 2020;98(1):54–66. doi:10.1111/imcb.12297, PMID:31625631.
[45] Zhang J, Du H, Shen M, Zhao Z, Ye X. Kangtaizhi Granule Alleviated Non-alcoholic Fatty Liver Disease in High-Fat Diet-Fed Rats and HepG2 Cells via AMPK/mTOR Signaling Pathway. J Immunol Res 2020;2020:3413186. doi:10.1155/2020/3413186, PMID:32884949.
[46] Pu T, Liao XH, Sun H, Guo H, Jiang X, Peng JB, *et al*. Augmenter of liver regeneration regulates autophagy in renal ischemia-reperfusion injury via the AMPK/mTOR pathway. Apoptosis 2017;22(7):955–969. doi:10.1007/s10495-017-1370-6, PMID:28466106.
[47] Yuan F, Xu Y, You K, Zhang J, Yang F, Li YX. Calcitriol alleviates ethanol-induced hepatotoxicity via AMPK/mTOR-mediated autophagy. Arch Biochem Biophys 2021;697:108694. doi:10.1016/j.abb.2020.108694, PMID:33232716.
[48] Chen QS, Shen A, Dai JW, Li TT, Huang WF, Shi K, *et al*. IL37 overexpression inhibits autophagy and apoptosis induced by hepatic ischemia reperfusion injury via modulating AMPK/mTOR/ULLK1 signalling pathways. Life Sci 2021;276:119424. doi:10.1016/j.lfs.2021.119424, PMID:33785334.